



Enhanced energy product in Y-Co-Fe magnets intermediate between Nd-Fe-B and ferrite

P. Tozman, M. Venkatesan, G. A. Zickler, J. Fidler, and J. M. D. Coey

Citation: [Applied Physics Letters](#) **107**, 032405 (2015); doi: 10.1063/1.4927306

View online: <http://dx.doi.org/10.1063/1.4927306>

View Table of Contents: <http://scitation.aip.org/content/aip/journal/apl/107/3?ver=pdfcov>

Published by the [AIP Publishing](#)

Articles you may be interested in

[Microstructural and magnetic properties of Nd-Fe-B alloys processed by equal-channel angular pressing](#)

J. Appl. Phys. **117**, 17A742 (2015); 10.1063/1.4918569

[Correlation of the energy product with evolution of the nanostructure in the Y,Dy,Nd-\(Fe, Co\)-B magnetic alloy](#)

J. Appl. Phys. **105**, 07A720 (2009); 10.1063/1.3067539

[Equiaxed Nd-Fe-B fine powder with high performance prepared by mechanical alloying](#)

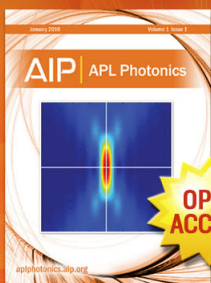
J. Appl. Phys. **101**, 09K502 (2007); 10.1063/1.2709408

[Microstructure and exchange coupling in nanocrystalline Nd₂\(FeCo\)₁₄B/ \$\alpha\$ -FeCo particles produced by spark erosion](#)

Appl. Phys. Lett. **86**, 122507 (2005); 10.1063/1.1890474

[Nanostructured NdFeB films processed by rapid thermal annealing](#)

J. Appl. Phys. **83**, 6611 (1998); 10.1063/1.367782



Launching in 2016!
The future of applied photonics research is here

AIP | APL
Photonics

Enhanced energy product in Y-Co-Fe magnets intermediate between Nd-Fe-B and ferrite

P. Tozman,¹ M. Venkatesan,¹ G. A. Zickler,² J. Fidler,² and J. M. D. Coey¹

¹*School of Physics and CRANN, Trinity College, Dublin 2, Ireland*

²*Institute of Solid State Physics, Vienna University of Technology, Vienna, Austria*

(Received 25 May 2015; accepted 10 July 2015; published online 21 July 2015)

The hysteresis of ball-milled Fe-doped YCo₅ powder has been optimized by controlling the temperature and time for rapid annealing under vacuum and argon. The crystallite size is only 25 nm; yet, it has been possible to field align Y(Co,Fe) powder with a 5–20 μm grain size in a 5 T field to obtain a remanence ratio of 0.65, due to texture in the ball-milled powder. The nominal energy product of the powder is 140 kJ/m³. A pressed magnet with 78% of theoretical density has an energy product of 65 kJ/m³. This magnet could fill the gap between oriented ferrite (34 kJ/m³) and oriented Nd-Fe-B (350 kJ/m³). © 2015 AIP Publishing LLC.

[<http://dx.doi.org/10.1063/1.4927306>]

There is increasing interest in finding oriented dense magnets with properties intermediate between sintered ferrite and sintered Nd-Fe-B, having reduced content of strategic rare earths.¹ Development and optimization of rare-earth-free magnets may be pursued by atomic substitutions in known uniaxial materials with reasonably high Curie temperatures (T_c) with a view to reducing materials' costs or improving processability. Fe-doped YCo₅ is a promising starting point for magnet development, because it is entirely free of the critical heavy rare earths, Tb and Dy; yttrium is potentially in surplus, and substitution of iron for cobalt on 3g (Co_{II}) sites should increase the saturation magnetization.² YCo₅ has the hexagonal CaCu₅-type structure (space group P 6/mmm) with lattice constants $a=494$ pm and $c=398$ pm.³ Bulk crystals have very strong uniaxial anisotropy with remanence $B_r=1.06$ T, Curie temperature $T_c=630$ °C, anisotropy constant $K_1=5.7$ MJ/m³, and anisotropy field $\mu_0 H_a=13.0$ T. The theoretical maximum energy product $(BH)_{MAX}=\frac{1}{4}\mu_0 M_s^2=224$ kJ/m³ at room temperature.^{4–6}

The magnetocrystalline anisotropy energy of YCo₅ comes mainly from the orbital moment of cobalt atoms in the structurally distorted 2c (Co_I) sites, which lie in the same plane as Y. Yttrium has no 4f electrons, but contributes to the anisotropy via its 4d electron which hybridizes with the 3d electrons of Fe or Co.^{7–10} The calculated magnetic anisotropy constant K_1 in YCo_{5-x}Fe_x increases with Fe doping from $x=0$ to $x=0.5$ and drops for larger x .¹¹ Experimental results confirm that K_1 first increases by 20% for $x=0.2$ and then decreases.^{3,8}

YCo_{5-x}M_x ($0\leq x\leq 0.75$) has been prepared in bulk, nanocomposites with (20 wt. % α Fe) and (30 wt. % Y₂Co₁₇), powders and nanoparticles with and without M=Fe, Cu doping by techniques such as arc-melting, mechanical milling, mechanochemical milling, and cluster deposition.^{3,8,12–18} Moreover, mechanically alloyed YCo₅ has a small temperature coefficient of coercivity and magnets made from it may be operable at high temperature.¹⁸

However, the best magnetic properties reported for conventional dry-milled and annealed YCo_{4.28} powder are

$\mu_0 H_C=1.6$ T and $(BH)_{max}=61$ kJ/m³.¹⁹ The nominal energy product of the powder has been increased to $(BH)_{max}=130$ kJ/m³ by mechanochemical milling with calcium in a process involving separation of the YCo₅ particles in a multi-step washing and magnetic alignment.²⁰

Here, YCo_{5-x}Fe_x ($0\leq x\leq 0.5$) alloy powders are prepared by high-energy ball milling and subsequent rapid thermal or vacuum annealing in order to obtain a good energy product. The effects of the two different annealing processes on magnetic and crystallographic properties are compared.

The YCo_{5-x}Fe_x alloys with $0\leq x\leq 0.5$ were prepared by arc melting in high-purity argon. The ingots were remelted four times to ensure homogeneity. Milling was then carried out under argon for 4 h in a Spex 8000 mixer/mill with stainless steel balls and a ball to powder charge ratio of 15:1. The as-milled YCo₅ powder was wrapped in Ta foil and then subjected to rapid thermal annealing under a flowing Ar with an infrared lamp (Ulvac-Riko MILA-5000) at temperatures (T_a) between 800 °C and 1050 °C for 1–5 min and cooled naturally. The iron-doped YCo_{5-x}Fe_x $0\leq x\leq 0.5$ powder samples were rapidly annealed at 800 °C for only 1–3 min, which was the optimum treatment to give the best energy product. The alternative, vacuum annealing treatment of the as-milled powders was carried out in a tube furnace preheated at 800 and 850 °C for 2–3 min under a vacuum of 10^{-6} – 10^{-7} Torr, followed by quenching. Ball-milled YCo_{4.8}Fe_{0.2} powder was pressed in a 5 mm die and vacuum annealed at 850 °C for 2 min. Structural characterization was carried out by X-ray diffraction (XRD) with a PANalytical X'Pert Pro diffractometer using Cu-K α radiation. Rietveld analysis of the diffraction patterns was performed using FullProf. The microstructure and composition were analysed with a scanning electron microscope (SEM Carl Zeiss Evo) and an analytical field emission transmission electron microscope (TEM FEI TECNAI F20), equipped with an energy dispersive X-ray detector (EDX) and a high angle annular dark field (HAADF) detector. Samples for room temperature magnetic measurements were prepared by mixing the annealed powder with Lecoset 7007 cold-curing resin inside

a 4 mm × 4 mm cylindrical Perspex bucket. Some samples were oriented in a 5 T field, and all the magnetic measurements were carried out using a 5 T Quantum Design superconducting quantum interference device magnetometer.

The XRD patterns of as-milled powders indicate a highly disordered crystal structure. However, rapidly annealed samples are mainly composed of the hexagonal CaCu_5 -type ($P6/mmm$) phase with a minor $\text{Th}_2\text{Zn}_{17}$ -type rhombohedral ($R\bar{3}m$) secondary phase.^{3,8} The XRD patterns of rapidly annealed powders (800 °C for 3 min) also show secondary rhombohedral Y_2Co_{17} . Fe-doping increases the lattice parameters and decreases the intensity of the hexagonal phase. According to our Rietveld refinement and an early neutron diffraction study,⁶ the Fe atoms prefer to occupy $2c$ Co_I sites rather than $3g$ Co_{II} sites. The lattice parameters increase from $a = 495$ pm and $c = 396$ pm to $a = 498$ pm and $c = 403$ pm, and the solid solubility limit is reached at $x = 0.3$.

Vacuum and rapid thermal annealed (850 °C, 2 min) samples are compared in Fig. 1. The peaks are broadened for the vacuum annealed sample and the main (111) peak overlaps with (200). The mean crystallite size for vacuum and rapid thermal annealed samples was found to be 11 nm and 65 nm, respectively, computed from the Scherrer broadening.

SEM images show that annealed samples were agglomerated in irregular shapes with a 10 μm average cluster size. The size and shape of the agglomerates are unaffected by annealing. Average grain sizes of 24 nm and 98 nm were determined for vacuum annealed (850 °C for 2 min) and rapid thermal annealed (850 °C for 2 min), respectively (Figs. 2(b) and 2(c)). The morphology of the as-milled sample is highly inhomogeneous with polycrystalline iron agglomerates, which are embedded in a nanocrystalline and mostly amorphous YCo_5 matrix with an average grain size of 8 nm. The average grain size obtained from TEM is always greater than that deduced from XRD, which can be attributed to the plastic deformation of bulk metallic particles.^{21,22} EDX analysis shows that the ratio of (Co + Fe) to Y was 5.7, in fair agreement with the nominal composition of 5.0.

Bulk YCo_5 shows insignificant coercivity at room temperature but a coercive ferromagnetic phase is obtained after

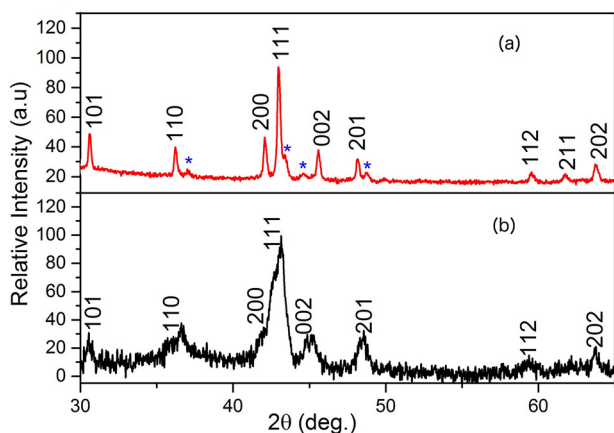


FIG. 1. XRD pattern for ball-milled rapid thermal (a) and vacuum annealed (b) at 850 °C for 2 min powders. Stars indicate the reflections of the secondary Y_2Co_{17} phase (300), (303), (006), and (223).

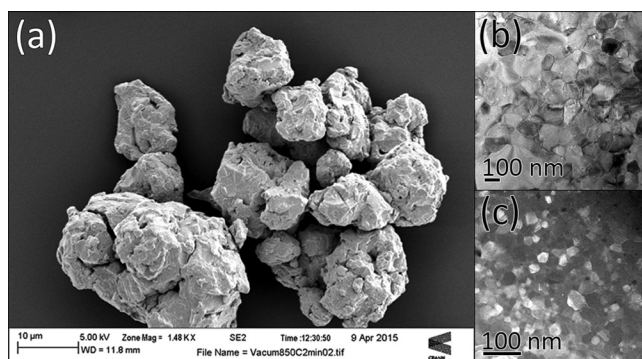


FIG. 2. SEM image of vacuum annealed (a) and TEM bright field image of rapid thermal annealed (850 °C for 2 min) $\text{YCo}_{4.8}\text{Fe}_{0.2}$ (b). STEM-HAADF image of vacuum annealed at 850 °C for 2 min $\text{YCo}_{4.8}\text{Fe}_{0.2}$ (c).

ball-milling and annealing. The coercivity $\mu_0 H_c$, saturation magnetization σ_{max} , and nominal maximum energy product $(BH)_{\text{max}}$ for the powder depend strongly on the annealing temperature, time, and Fe-doping. None of the annealed powder samples was saturated under 5 T.

YCo_5 powders were then rapidly annealed for 1 min at temperatures ranging from 800 to 1050 °C at 50 °C intervals. Coercivity decreases from 0.83 T to 0.55 T with increasing temperature, except at 900 °C where it is 0.88 T. The coercivity also decreases with increasing annealing time from 1

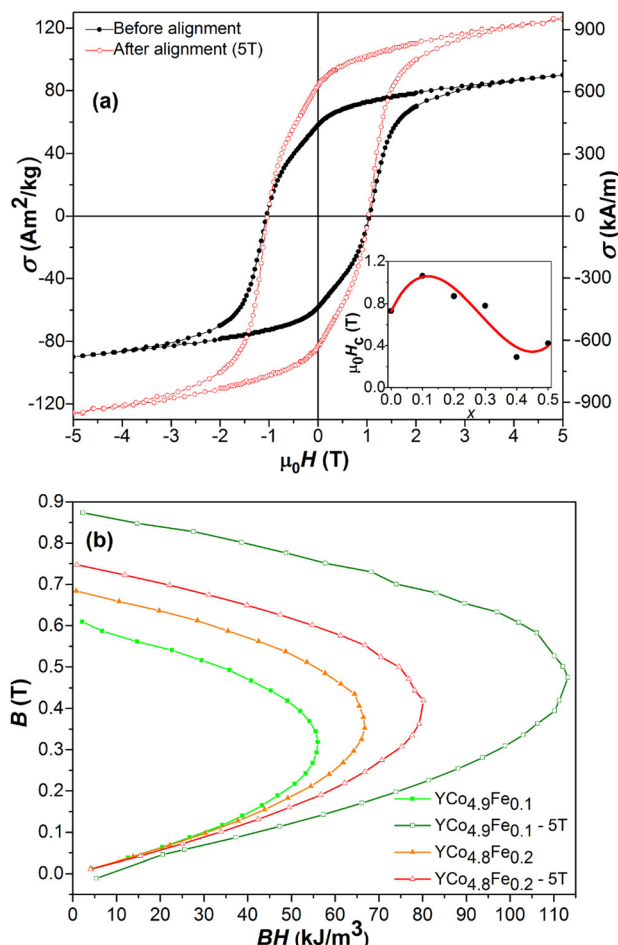


FIG. 3. Hysteresis of rapid thermal annealed $\text{YCo}_{4.9}\text{Fe}_{0.1}$ before and after magnetic alignment (a). Calculated maximum energy product before and after magnetic alignment (b).

to 5 min at 800 °C; the best powder energy product of 66 kJ/m³ for 2 min annealing was deduced assuming crystallographic density $\rho = 7560 \text{ kg/m}^3$ and $\mathcal{N} = 1/3$ for spherical powders.

Ball-milled $\text{YCo}_{5-x}\text{Fe}_x$ with $0 \leq x \leq 0.5$ was then rapidly thermally annealed at 800 °C for 1–3 min, and the highest coercivity and $(BH)_{\text{max}}$ were obtained for 2 min. $\text{YCo}_{4.9}\text{Fe}_{0.1}$ has the best magnetic properties with $\mu_0 H_c = 1.06 \text{ T}$, $(BH)_{\text{max}} = 56 \text{ kJ/m}^3$, and $\sigma_{\text{max}} = 90 \text{ Am}^2/\text{kg}$.

These properties were improved by magnetically aligning the powder in epoxy resin under 5 T; the value of $(BH)_{\text{max}}$ increases up to 114 kJ/m³ due to an increment of σ_{max} to 128 Am²/kg and $\sigma_r/\sigma_{\text{max}} = 0.65$. The magnitude of $\mu_0 H_c$ decreases, whereas the value of σ_{max} is enhanced with Fe-doping, in agreement with calculations.² After reaching the solid solubility limit $x = 0.3$, the coercivity drops significantly as shown in Fig. 3(a). Unlike dry-ball milled La(Co,Fe) powders, there is no step in the demagnetization curve near zero field.²³

The best magnetic properties were obtained after a short vacuum anneal at 850 °C for 2 min. The coercivity falls from 1.0 T to 0.42 T as x changes from 0 to 0.5, with a sharp decrease when $x \geq 0.3$.

The highest $(BH)_{\text{max}}$, obtained for $\text{YCo}_{4.8}\text{Fe}_{0.2}$, powders dispersed in epoxy is 81 kJ/m³ with $\sigma_{\text{max}} = 112 \text{ Am}^2/\text{kg}$ and

$\mu_0 H_c = 0.75 \text{ T}$ with $\mathcal{N} = 1/3$. After alignment in 5 T, the powder value of $(BH)_{\text{max}}$ is 140 kJ/m³ with $\sigma_r/\sigma_{\text{max}} = 0.65$ (Fig. 4) due to the enhanced 5 T magnetization of 144 Am²/kg. Alignment increases the magnetization by 30% for $x = 0.3$ and $x = 0.2$. For other compositions, it is less, 5%–10%. The coercivity for magnetically aligned $\text{YCo}_{4.8}\text{Fe}_{0.2}$ decreases only by 13% from 0.75 T, its room temperature value, at 400 K demonstrating good temperature stability. The best magnetic properties obtained by rapid thermal annealing under similar conditions (850 °C 2 min) are $(BH)_{\text{max}} = 51 \text{ kJ/m}^3$, $\mu_0 H_c = 0.83 \text{ T}$, and $\sigma_{\text{max}} = 95 \text{ Am}^2/\text{kg}$.

The powder of $\text{YCo}_{4.8}\text{Fe}_{0.2}$ was pressed into a pellet and sintered in preheated furnace at 850 °C for 2 min under vacuum. The density of the sintered ingot is $\rho = 5880 \text{ kg/m}^3$. The room temperature coercivity is unchanged. The maximum energy product is 66 kJ/m³, computed with $\mathcal{N} = 0.875$, corresponding to the pellet shape.²⁴ The variation of $(BH)_{\text{max}}$ with different \mathcal{N} values is compared in Figure 5(b).

We have increased the energy product of $\text{YCo}_{4.8}\text{Fe}_{0.2}$ powder to 140 kJ/m³ without calcium, in optimized annealing conditions with magnetic alignment. Surprisingly, although the individual crystallite size is only 25 nm, it was possible to obtain a 30% increment in remanence by aligning 10–50 μm powders. This implies a significant crystallographic [001] texture in the ball-milled material. The

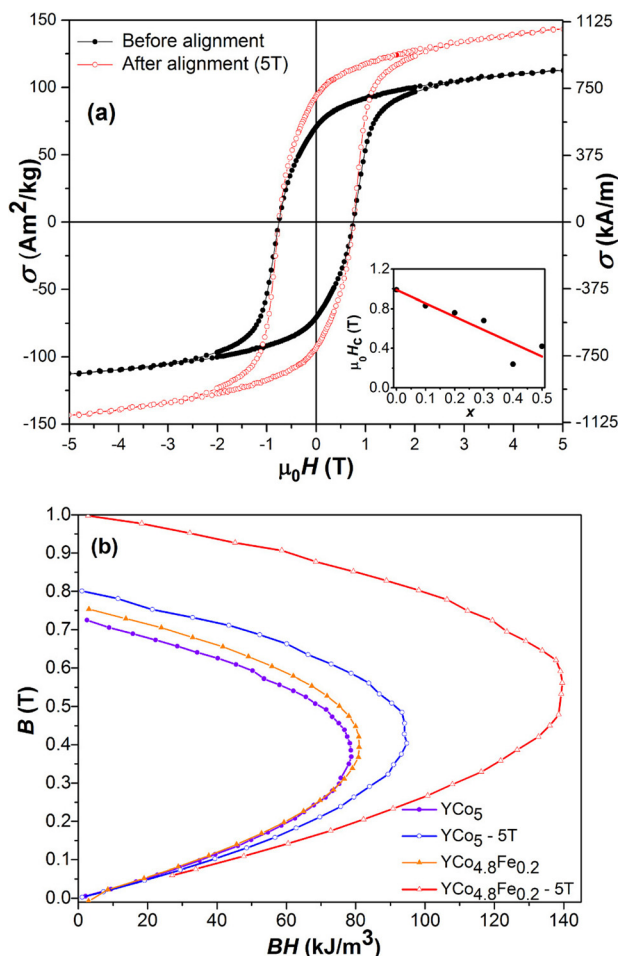


FIG. 4. Vacuum annealed $\text{YCo}_{4.8}\text{Fe}_{0.2}$ at 850 °C for 2 min before and after magnetic alignment (a) and calculated $(BH)_{\text{max}}$ of $\text{YCo}_{5-x}\text{Fe}_x$ powders before and after magnetic alignment (b).

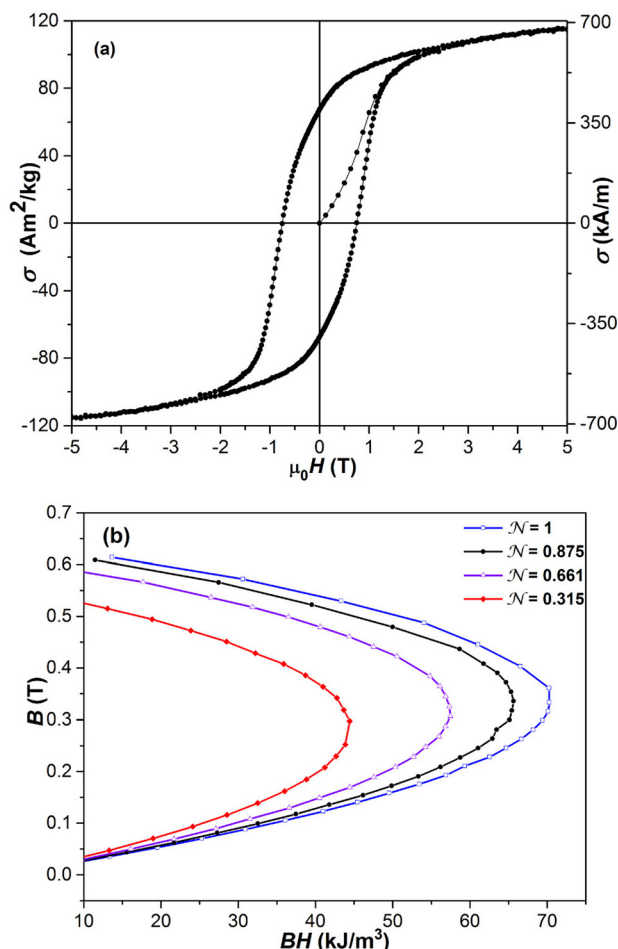


FIG. 5. Hysteresis of vacuum annealed pressed magnet $\text{YCo}_{4.8}\text{Fe}_{0.2}$ (a). Calculated maximum energy product for different demagnetizing factors \mathcal{N} , for $\rho = 5880 \text{ kg/m}^3$ (b).

nanocrystal axes are not randomly aligned, but a significant uniaxial texture is imparted by ball-milling. The textured powder can be field aligned, leading to remanence enhancement. Since the coercivity is controlled by microstructure, it is expected that a similar energy product to that measured on powder should be found in fully dense aligned magnets.

This work was supported by the EU FP7 ROMEO Project. TEM investigation was carried out at the University Service Centre for Transmission Electron Microscopy, Vienna University of Technology, Austria.

- ¹J. M. D. Coey, *IEEE Trans. Magn.* **47**, 4671 (2011).
- ²X. B. Liu, Z. Altounian, and M. Yue, *J. Appl. Phys.* **107**, 09A718 (2010).
- ³B. Das, B. Balamurugan, W. Y. Zhang, R. Skomski, E. S. Krage, S. R. Valloppilly, J. E. Shield, and D. J. Sellmyer, in Proceeding of the 22nd International Workshop on Rare-Earth Permanent Magnets and their Applications (REPM'12), Nagasaki, Japan, 2-5 September 2012, article **P3-025**, p. 427, available at <http://digitalcommons.unl.edu/physicsskomski/89/>.
- ⁴K. J. Strnat and R. M. W. Strnat, *J. Magn. Magn. Mater.* **100**, 38 (1991).
- ⁵G. Hoffer and K. Strnat, *IEEE Trans. Magn.* **2**, 487 (1966).
- ⁶J. M. Alameda, J. Deportes, D. Givord, R. Lemaire, and Q. Lu, *J. Magn. Magn. Mater.* **15**, 1257 (1980).
- ⁷G. H. O. Daalderop, P. J. Kelly, and M. F. H. Schuurmans, *Phys. Rev. B* **53**, 14415 (1996).
- ⁸J. Deportes, D. Givord, J. Schweizer, and F. Tasset, *IEEE Trans. Magn.* **12**, 1000 (1976).
- ⁹L. Steinbeck, M. Richter, and H. Eschrig, *J. Magn. Magn. Mater.* **226**, 1011 (2001).
- ¹⁰D. Givord and D. Courtois, *J. Magn. Magn. Mater.* **196**, 684 (1999).
- ¹¹P. Larson, I. I. Mazin, and D. A. Papaconstantopoulos, *Phys. Rev. B* **69**, 134408 (2004).
- ¹²J. L. Sánchez Ll, J. T. Elizalde-Galindo, and J. A. Matutes-Aquino, *Solid State Commun.* **127**, 527 (2003).
- ¹³J. T. Elizalde Galindo, C. E. Botez, F. Rivera Gómez, and J. A. M. Aquino, *Phys. Lett. A* **366**, 110 (2007).
- ¹⁴J. T. Elizalde-Galindo, A. W. Bhuiya, F. Rivera Gómez, J. A. M. Aquino, and C. E. Botez, *J. Phys. D: Appl. Phys.* **41**, 095008 (2008).
- ¹⁵J. Sanchez Ll, B. Hernando, M. J. Pérez, and J. D. Santos, *J. Non-Cryst. Solids* **353**, 835 (2007).
- ¹⁶B. Balasubramanian, R. Skomski, X. Li, S. R. Valloppilly, J. E. Shield, G. C. Hadjipanayis, and D. J. Sellmyer, *Nano Lett.* **11**, 1747 (2011).
- ¹⁷J. C. Téllez-Blanco, R. Grössinger, R. Sato Turtelli, and E. Estévez-Rams, *IEEE Trans. Magn.* **36**, 3333 (2000).
- ¹⁸I. A. Al-Omari, R. Skomski, R. A. Thomas, D. Leslie-Pelecky, and D. J. Sellmyer, *IEEE Trans. Magn.* **37**, 2534 (2001).
- ¹⁹N. Tang, Z. Chen, Y. Zhang, G. C. Hadjipanayis, and F. Yang, *J. Magn. Magn. Mater.* **219**, 173 (2000).
- ²⁰A. M. Gabay, X. Hu, and G. C. Hadjipanayis, *J. Magn. Magn. Mater.* **368**, 75 (2014).
- ²¹T. Ungár, G. Tichy, J. Gubicza, and R. J. Hellmig, *Powder Diffr.* **20**, 366 (2005).
- ²²Y. Zhong, D. Ping, X. Song, and F. Yin, *J. Alloys Compd.* **476**, 113 (2009).
- ²³P. Tozman, M. Venkatesan, and J. M. D. Coey, *IEEE Trans. Magn.* **50**, 1 (2014).
- ²⁴D.-X. Chen, E. Pardo, and A. Sanchez, *IEEE Trans. Magn.* **38**, 1742 (2002).